

# Galvanic Skin Response and AE-LSTM for Anomaly Detection in VR-Induced Motion Sickness

Wadhah Al-ashwal, Houshyar Asadi, *Member, IEEE*, Mohammadreza Chalak Qazani, Shady Mohamed, and Saeid Nahavandi, *Fellow, IEEE*, Bernhard E. Riecke

**Abstract**—This study advances the understanding of motion sickness (MS) by integrating subjective measures, like the simulator sickness questionnaire (SSQ), with objective physiological metrics, particularly galvanic skin response (GSR), analysed through an Autoencoder Long Short-Term Memory (AE-LSTM) model. This model, designed for unsupervised anomaly detection, evaluates GSR data to detect differences in physiological (GSR) responses to conditions of different MS potential (here different weather scenarios in a naturalistic VR helicopter simulation). By comparing these physiological anomalies with self-reported cybersickness scores, our findings highlight the importance of combining machine learning-analysed physiological data with subjective reports, offering a comprehensive approach to assessing MS in different conditions. The transition from clear to stormy scenarios revealed marked elevations in MS scores, although the model was currently not able to reliably identify scenario-specific physiological responses that correlate with increased MS.

**Keywords**— *Cybersickness, VIMS, SSQ, GSR*

## I. Introduction

The occurrence of motion sickness (MS) in the real world is usually associated with an actual physical motion. However, when it is induced by visual stimuli alone without any actual motion of the observer, it is known as visually induced motion sickness (VIM[1]–[3]) Motion sickness can manifest in a broad spectrum of symptoms, beginning with subtle physiological changes like alterations in skin tone, body temperature, and salivation, and progressing to overt discomfort, including headaches, nausea, and dizziness. In rare cases, it can even escalate to more serious symptoms such as vomiting [1], [3]–[7].

The prevalence of VIMS is reported to be highly variable (ranges from 1-95% [8], [9]), influenced by numerous factors such as the design of virtual reality (VR) equipment and the nature of the visual content and the dynamics of simulated self-motion, as well as participant factors. The health implications of VIMS are multifaceted, presenting differently across various VR platforms and contexts. This variability

spans a spectrum from video game sickness to simulator sickness, cybersickness, and VR sickness, each distinguished by the context of use [10] [11].

Although virtual reality (VR) systems have seen substantial enhancements and have been effectively applied in various contexts, they have not yet reached the expected level of adoption as a consumer-grade technology. The introduction of head-mounted displays (HMDs) has brought about a specific kind of motion sickness referred to as cybersickness. Contributing factors especially for HMDs are functional challenges like latency, where there is a delay between a user's actual head movements and the corresponding updating of the visuals, poor illumination, poor contrast and length of exposure to VR contributing to cybersickness [12][13].

In the study conducted by Irmak et al. [14], there was a noticeable variation in galvanic skin response (GSR) in relation to motion sickness. Notably, both tonic and phasic GSR exhibited substantial increases, showing a clear correlation with the severity of motion sickness. Wan et al. [15] recorded skin-conductance responses (both phasic and tonic) and observed that as the duration of stimuli exposure increased, both the subjective ratings of motion sickness and skin conductance levels also increased. This makes skin conductance a sensitive physiological indicator of motion sickness induced by visual stimuli. This research builds upon existing knowledge to investigate the relationship between galvanic skin response (GSR) and the intensity of motion sickness (MS), with a particular emphasis on the role played by different environmental factors, such as weather conditions.

The choice of environmental factors, particularly clear and stormy weather conditions, for investigation in this study is grounded in their pronounced variability and potential to significantly alter the visual and physical experiences of VR users. Clear weather conditions provide a baseline for understanding the normative physiological response to motion in an unobstructed environment, offering a control scenario against which the effects of more adverse conditions can be measured. In contrast, stormy weather introduces visual disturbances, such as reduced visibility and dynamic visual patterns, along with increased physical turbulence. These factors are hypothesized to intensify the sensory conflict that contributes to motion sickness, thereby amplifying galvanic skin response (GSR) as an indicator of physiological arousal and discomfort. By examining these distinct scenarios, the study aims to dissect the impact of environmental visual and physical stressors on motion sickness, providing insights into the mechanisms underlying GSR variability in response to motion. This exploration is particularly relevant for improving the design and safety of

---

Research supported by Australian Research Council (ARC).

W. Al-ashwal. is with the Institute for Intelligent Systems Research and Innovation (IISRI), Deakin University, Australia (e-mail: [walashwal@deakin.edu.au](mailto:walashwal@deakin.edu.au)).

H. Asadi, S. Mohammed (e-mail: [houshyar.asadi@deakin.edu.au](mailto:houshyar.asadi@deakin.edu.au); [shadym@deakin.edu.au](mailto:shadym@deakin.edu.au)) are with the Institute for Intelligent Systems Research and Innovation, Deakin University, Geelong, VIC 3125, Australia. M.R.Chalak Qazani is with Faculty of Computing and Information Technology, Sohar University, Sohar, Oman ([m.r.chalakqazani@gmail.com](mailto:m.r.chalakqazani@gmail.com)). S. Nahavandi is with Swinburne University of Technology, Hawthorn, VIC 3122, Australia ([snahavandi@swin.edu.au](mailto:snahavandi@swin.edu.au)); B. E. Riecke ([ber1@sfu.ca](mailto:ber1@sfu.ca)) is with the School of Interactive Arts & Technology (SIAT); Simon Fraser University, Surrey, BC V3T 0A3, Canada;



Figure 1: Clear weather (left) and stormy weather (right)

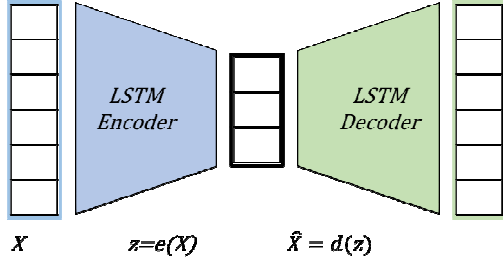


Figure 2: A simplified block diagram of an auto-encoder [16]

simulation technologies and transport systems, where understanding the interplay between

environmental conditions and motion sickness can lead to enhanced user experiences and mitigation strategies.

To tackle this objective, we designed a helicopter simulation, crafting a range of aerial scenarios with varying weather conditions to establish a controlled yet ecologically valid environment for the study. This approach was taken to evaluate the influence of these elements on GSR as a measure for motion sickness [17,18].

The study explores the relationship between motion sickness (MS) and physiological responses, notably galvanic skin response (GSR), driven by the need to mitigate MS's adverse effects on the physiological system. This exploration is driven by the urgency to mitigate the adverse impacts of motion sickness (MS), which include reduced well-being and productivity due to discomfort and nausea, posing a significant barrier to the effective use of VR in a multitude of applications. Recognizing GSR as a measurable indicator of MS, our research aims to enable the development of strategies to predict and alleviate MS, especially in contexts prone to inducing it, such as travel and VR simulations. Uncovering these physiological markers is a crucial step towards advancing the management and reduction of impacts.

## II. Research Materials and Methods

Prior research in the field has utilised various computational models to analyse the physiological correlates of motion sickness, with methods ranging from simple statistical regressions to more complex neural networks. For example, the authors in [19] used collected data from 15 participants with a total of 11 tests for each user and used FlowNet optical flow algorithm to estimate MS level via vection. The correlation coefficient of this study was negative and did not reflect a significant correlation with the MS score. Ko et al. [20] used a support vector machine (SVM) classifier for their learning model. EEG data for 6 participants were used to estimate MS level. The model achieved an accuracy of 59% - 97%. The study

in [21] demonstrates that a deep learning-based approach, specifically using an LSTM model, can effectively predict VR sickness using postural instability as a measure in users navigating immersive virtual environments.

In this study, we investigate the potential of anomaly detection capability of LSTM autoencoder to detect the changes in physiological data, in this case GSR, associated with different VR scenarios.

### A. Autoencoder-Long Short-Term Memory

The Long Short-Term Memory (LSTM) model is fully equipped to process time series and handle time lags between inputs. It is able to remember values pertaining to any length of time stamp [22] by adding a ‘‘gate’’ to the cell. The LSTM architecture is shown in Figure 2. It can be expressed mathematically as follows:

$$\begin{aligned}
 i_t &= \sigma(W_{ih}h_{t-1} + W_{ix}x_t + b_i), \\
 \tilde{c}_t &= \tanh(W_{ch}h_{t-1} + W_{cx}x_t + b_c), \\
 c_t &= c_{t-1} + i_t \otimes \tilde{c}_t, \\
 o_t &= \sigma(W_{oh}h_{t-1} + W_{ox}x_t + b_o), \\
 h_t &= o_t \otimes \tanh(c_t),
 \end{aligned} \tag{1}$$

where  $i_t$ : input/update gate's activation vector,  $x_t$ : input vector to the LSTM unit,  $h_t$ : hidden state vector,  $\sigma$ : activation function,  $o_t$ : output gate's activation vector,  $c_t$  and  $\tilde{c}$  are the encoded and decoded state vectors, while  $\otimes$  is elementwise (pointwise) product operator.  $W_{iz}$ ,  $W_{ix}$ ,  $W_{oz}$ ,  $W_{ox}$  and  $W_{cx}$  are the weights, and  $b$  is the bias vector.

The features of LSTM eliminate the need for pre-determined time windows required by traditional techniques to detect changes in a sequence of long-term dependencies. It allows the LSTM network to work well on capturing the behaviour of time series sequences. This has led to the use of LSTM in detecting anomalous sequences in time series, which is generally denoted as Anomaly detection (AD) [23]–[26].

To realise AD, a machine learning (ML) prediction model is trained to recognise normal behaviours. Given a new input, the prediction error generated by the trained ML model is utilised to detect abnormal behaviours [23]. AD techniques have been used to identify anomalies from time series data in many areas, e.g. supply chain management (SCM), machinery, and finance. [16].

A standard auto-encoder consists of two main parts: encoder and decoder. The encoder compresses the data samples into short representations and propagates them to a latent space. The decoder neural network then decompresses the codes into representations as closely to the original ones as possible [27]. The output is compared with the original data sample to generate an error estimate [16]. By compressing the data samples into smaller representations, the auto-encoder is able to capture the most important features while reducing the data dimensions. By embedding auto-encoders into LSTMs, they can inherit the ability of LSTMs to learn and store features over long sequences. This capability makes the resulting method useful for detecting

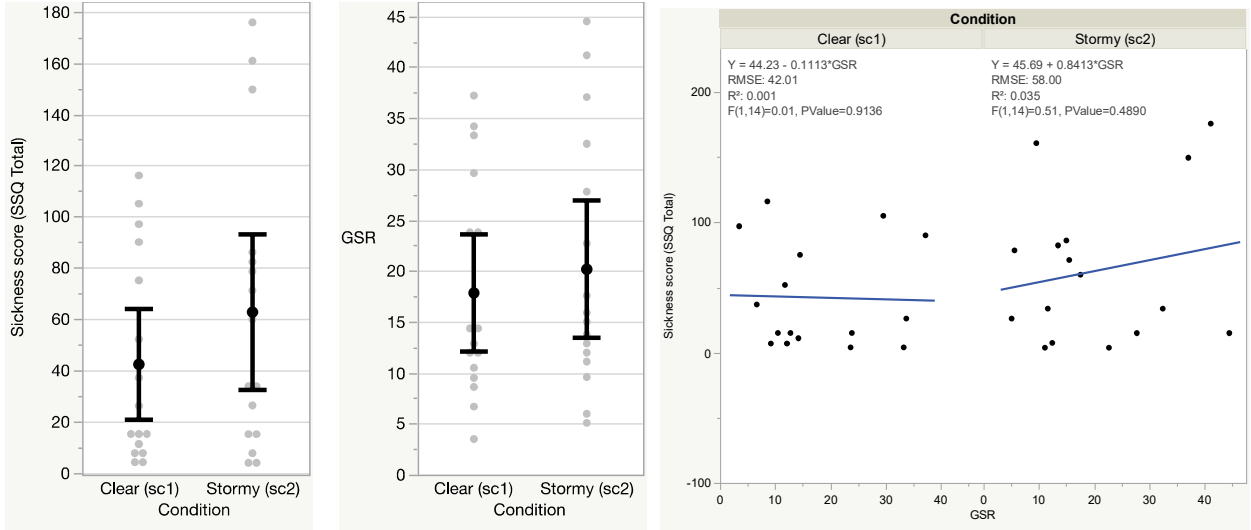


Figure 3: Comparative analysis of the total sickness score (SSQ total, left) and the GSR values (middle) averaged over the exposure duration, for the clear and stormy weather scenarios. Depicted are mean and 95% confidence intervals. Gray dots depict individual participant values, illustrating the large between-participant variability in both introspective and physiological data. Right: linear correlations between the total sickness scores and GSR values, separately for each condition.

anomalies in multivariate time series data. Figure 2 depicts a simplified block diagram of the auto-encoder workflow.

The auto-encoder reconstructs the input vectors  $X_1, \dots, X_m$  to become the outputs  $\hat{X}_1, \dots, \hat{X}_m$  such that  $h_{W,b}(x) \approx x$ , where  $W$  and  $b$  are the weight and bias vector, respectively, while keeping the reconstruction error as minimum as possible, therefore setting up a threshold. The error magnitude

is the result of comparing the auto-encoder output with the initial data sample, which is then passed to the network for the weights to be updated [16]. During the training process, the auto-encoder learns to minimise the reconstruction error [28], as defined in Eq. 2

$$\text{Error}(i) = \sqrt{\sum_{j=1}^D \|x_j(i) - \hat{x}_j(i)\|^2} \quad (2)$$

where  $x(i)$ : normal training data set,  $D$ : vector of  $D$  different variables) and  $\hat{x}(i)$ : output (reconstructed) data set.

The training process halts when the reconstruction error reaches its minimum, signifying that the model has optimized its ability to replicate the input data. At this juncture, the lowest loss value observed during training is earmarked as a benchmark. Any subsequent errors exceeding this benchmark are flagged as potential anomalies. This calibrated threshold, rooted in the model's most efficient performance, equips the system to identify deviations in new data—specifically, abrupt changes in amplitude that diverge from established norms. Thus, with the threshold set based on minimal loss error, the model stands primed to detect anomalous sequences in incoming data.

To detect the changes of GSR response to the change in weather scenarios, we present a system designed for unsupervised anomaly detection employing the capabilities of LSTM autoencoders. This system addresses a critical gap

in physiological data analysis, particularly in scenarios where labelled anomaly data is scarce or unavailable.

This critical gap in physiological data analysis, especially regarding GSR, lies in the challenge of detecting nuanced physiological changes without access to extensive labelled datasets for supervised learning. This is particularly problematic in contexts like evaluating the impact of varying weather scenarios, where specific patterns of anomalies are subtle and labelling data for anomalies is often impractical. To bridge this gap, we introduce a system utilizing LSTM autoencoders for unsupervised anomaly detection. By learning the normal patterns of GSR data, our system can identify deviations without needing pre-labelled anomaly data, thus offering a novel approach to analyse physiological responses in conditions where labelled data is scarce. This methodology not only circumvents the limitations posed by the lack of labelled datasets but also enables a deeper understanding of physiological responses to environmental changes, marking a significant advancement in the field. Our methodology recognizes the unique nature of GSR data, acknowledging that it can reflect substantial individual variability and is sensitive to differing scenarios/contexts. Therefore, our system is uniquely tailored to process and analyse data on a participant-specific basis, providing an accurate identification of anomalies.

The model is trained exclusively on 'normal' GSR data (Scen1/clear weather in our case) for each participant, enabling it to learn and internalise the typical physiological patterns exhibited under standard conditions. Post-training, the model is tasked with reconstructing both normal and presumed 'abnormal' (Scen2/stormy weather) data. Anomalies are detected by quantifying the reconstruction error, where larger errors signal significant deviations from the learned normal patterns, flagging potential anomalies.

A key benefit of our approach is its adaptability and scalability. The system is designed to handle multiple participants, acknowledging the inherent variability in human physiological responses. Through individualized model training, the system effectively accounts for this variability,

ensuring that the detection of anomalies is both precise and reliable. During validation, the model is first validated on unseen normal data to ascertain its reconstruction accuracy, and subsequently on abnormal data to evaluate its anomaly detection ability.

For scalability and adaptability to multiple participants, we encapsulated core functionalities into modular functions. These include functions for data loading and preprocessing, model building and training, and anomaly detection, which calculates reconstruction errors to identify anomalies. The system iterates over each participant's data, applying these functions systematically, thereby maintaining consistency across different datasets.

### B. Procedure and Experimental Setup

The study involved 16 male volunteers, ages ranging from 18 to 45. The study was conducted in strict adherence to COVID-19 safety protocols, with approval from Deakin University's Ethic Committee (reference number: SEBE-2020-23HEAG). Participants underwent COVID-19 screening, received a brief explanation of plain language statement (PLS) and signed a consent form. Before the experiment, participants completed a pre-SSQ (Simulator Sickness Questionnaire by Kennedy et al. [29]) to get a baseline MS assessment. Participants engaged in a brief, 10-minute training session, divided equally between flatscreen and head-mounted display (HMD) training, to familiarize them with the basics of flying and operating the helicopter simulator. The experiment included four distinct weather scenarios in the simulator in randomised order - clear, broken, stormy, and AI-controlled conditions. Each scenario lasted up to 7 minutes. However, this study focuses on results from the clear and stormy conditions. Figure 1 shows screenshots of the clear and weather conditions in Xplane11.

Participants were assigned flying scenarios in a randomized order. Their objective was to pilot the simulator in a pattern resembling a number 8 motion. After each scenario, participants completed a post-SSQ (Simulator Sickness Questionnaire). The galvanic skin response (GSR) data were recorded using Equivocal EQ02 life monitor, a multi-parameter device which is used to monitor the physiological data.

## III. RESULTS AND DISCUSSION

### A. Statistical Analysis

Pre-SSQ results indicated that none of the participants reported discomfort before commencing the experiments, ensuring initial conditions were uniform. All individuals successfully completed simulations under clear weather conditions. However, simulations under stormy conditions led to two participants discontinuing due to elevated cybersickness.

The total motion sickness score in this study was evaluated using the SSQ by Kennedy et al. [29]. Figure 2 (left) presents a comparison of the total sickness (TS) scores for participants exposed to clear and stormy weather scenarios in the helicopter simulator study. Results indicate a significant increase in total SSQ scores from the clear weather condition ( $M = 42.25$ ,  $SD = 40.6$ ) to the stormy condition ( $M = 62.64$ ,  $SD = 57.04$ ,  $t(15) = -2.27$ ,  $p = 0.0386$ ). This indicates that participants experienced more severe motion sickness symptoms under stormy conditions than in

clear weather, highlighting the impact of environmental variability on motion sickness severity. The data plot also illustrates the large between-participant differences in experiences sickness in both environments, and how the stormy condition yielded the higher sickness ratings.

Figure 3 (middle) shows a similar plot for participants' GSR values averaged over the duration of each trial. Overall the stormy condition resulted in significantly higher GSR values ( $M = 20.15$ ,  $SD = 12.65$ ) than the clear sky condition ( $M = 17.82$ ,  $SD = 10.77$ ,  $t(15) = 2.36$ ,  $p = 0.0325$ ). However, as indicated in Figure 4 (right) there were no significant correlations between participants' mean GSR values and the reported motion sickness for either the clear sky condition ( $p = .91$ ) or the stormy condition ( $p = .49$ ), suggesting that the GSR values by themselves are not a reliable indicator of experienced motion sickness.

### B. Model Evaluation and Outcome

Our machine learning model was implemented to capture the changes of GSR values with reference to the changes in weather conditions. Figure 4 illustrates the reconstruction error for one participant as an example. This plot displays the reconstruction error for each sequence in the dataset. The red line represents the threshold for anomaly detection. Sequences that have a reconstruction error above this threshold are considered anomalous. The relatively consistent occurrence of peaks above the threshold suggests that the model can identify sequences that deviate from the 'normal' pattern it learned during training. These are the points of interest that might correspond to anomalous events or states in the GSR data as discussed below.

Figure 5 top plot (normal data) shows the reconstruction error over a sequence of data points under normal (clear sky) conditions for a representative participant (P16). The reconstruction error is generally low, which is expected as the model was trained on this type of data. Towards the end of the sequence, there is a noticeable increase in error, with several peaks that have been highlighted as anomalies (red dots). These peaks indicate sequences where the GSR data deviated from the learned normal pattern to a degree that exceeded the predefined anomaly threshold. It's possible that these could be false positives or could indicate subtle changes in the physiological state not captured during training. It could also indicate that P16 experienced more motion sickness towards the end of the trial, as is common for extended VR exposures.

Figure 6 bottom plot (abnormal data) shows the reconstruction error for the same participant plotted for what is assumed to be data under abnormal (stormy weather) conditions. Overall reconstruction error seems slightly elevated compared to the normal data as can be expected as the model was trained on the normal data only. However, the number of detected anomalies seems fairly comparable between the normal (clear) and abnormal (stormy) conditions. To investigate this further, we compared the number of anomalies detected by our model for each participant and condition in Figure 5 (left). This analysis illustrates how the number of anomalies detected was quite similar and not significantly different between the clear sky (normal) condition ( $M = 15.75$ ,  $SD = 6.30$ ) and stormy weather (abnormal) condition ( $M = 15.44$ ,  $SD = 5.29$ ,  $t(15) = -0.22$ ,  $p = 0.83$ ). Figure 6 (right) illustrates the lack of any significant correlation between the number of detected

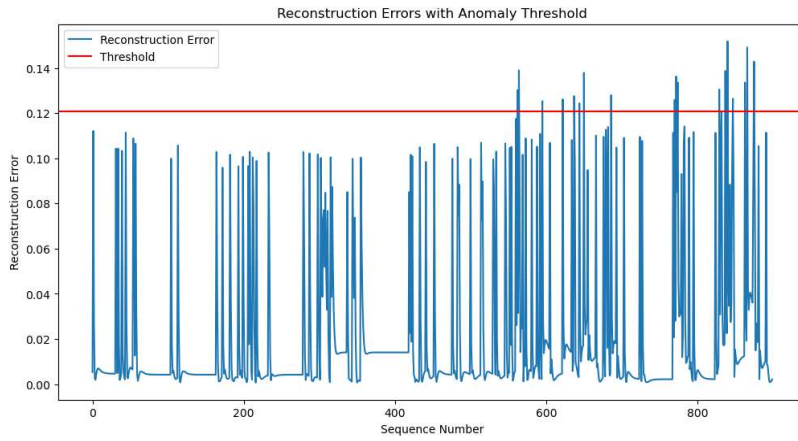


Figure 4: Reconstruction error distribution with anomaly threshold. The chart displays the reconstruction error for each sequence of one participant (1 sequence = 2 sample/sec × 60 sec = 120 samples) in the dataset, with the red horizontal line marking the threshold above which points are classified as anomalies. Peaks above the line represent sequences that significantly diverge from the model's learned patterns, indicating potential anomalies.

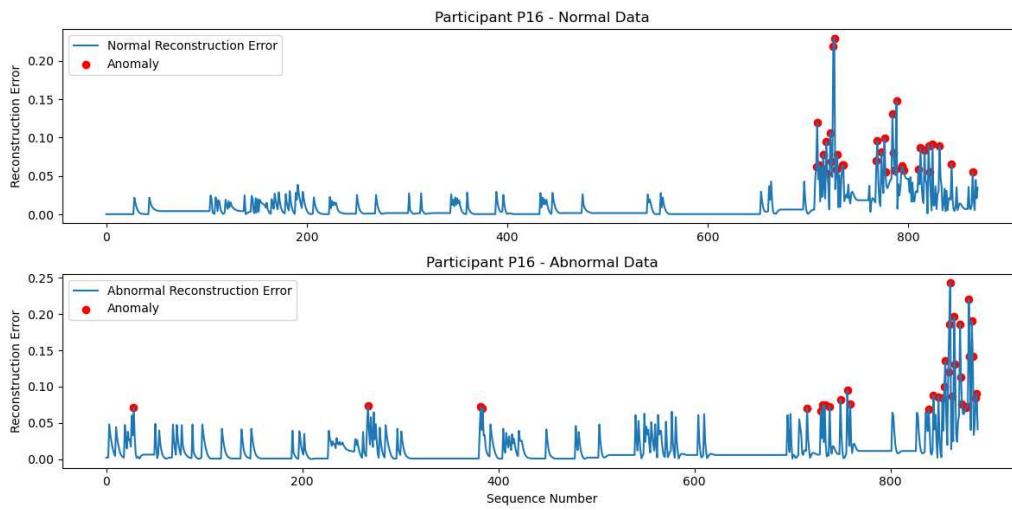


Figure 5: Testing the model reconstruction error with new data (participant P16's normal (clear) and abnormal (stormy) GSR data)

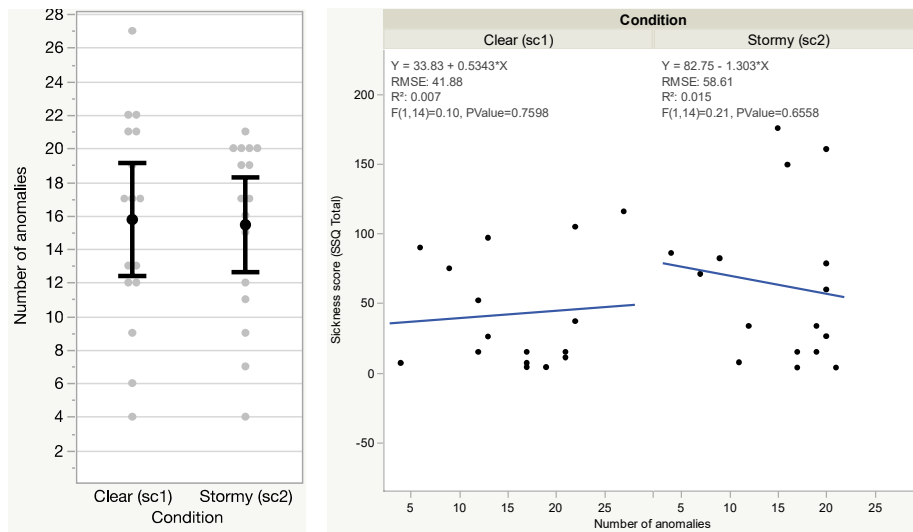


Figure 6: Left: Comparison of the number of anomalies detected by our model per condition, showing mean and 95% confidence intervals, with grey dots indicating individual participant values. Right: linear correlations between the total sickness scores and number of anomalies detected, separately for each condition.

anomalies and the reported sickness scores for either the clear sky (normal) condition ( $p = .76$ ) or the stormy (abnormal) condition ( $p = .66$ ), suggesting that the detected number of anomalies by themselves are not a reliable predictor of experienced motion sickness.

Further research is needed to better understand the nature and potential meaning of these anomalies, potentially with domain expertise, to determine their potential significance and whether they correspond to true/meaningful physiological events or other factors.

Subsequent analyses may incorporate a multifaceted assessment strategy, cross-referencing GSR data with other physiological measures such as heart rate variability or EEG. Such a multidimensional approach could enhance the detection of subtle physiological responses to motion sickness.

that are not apparent through GSR alone. It also opens the possibility of discovering biomarkers that are more consistently predictive of motion sickness, laying the groundwork for a composite physiological profile of VR-induced discomfort.

#### IV. CONCLUSIONS

Drawing on extensive research into visually induced motion sickness (VIMS) and its physiological correlates, this study has deployed advanced machine learning techniques to probe the potential relationship between galvanic skin response (GSR) and varying intensities of motion sickness in virtual reality scenarios. Utilizing an LSTM autoencoder, renowned for its proficiency in time series analysis and anomaly detection, we have developed a system that can capture shifts in GSR, and investigated if those might be indicative of motion sickness experienced across different environmental conditions simulated in a VR helicopter flight.

Our system's architecture, designed to accommodate the individual variability inherent in physiological responses, has been pivotal in reliably detecting anomalies. Trained on normal GSR data under clear weather conditions, the model demonstrated its capability to learn and replicate normal physiological patterns. When tasked with reconstructing data from both clear and stormy weather scenarios, the model's reconstruction errors served as a reliable metric for identifying significant deviations from these patterns. However, the interpretation of these errors as reliable metrics for identifying significant deviations in motion sickness requires further validation.

While the current study did not establish significant correlations between the incidence of motion sickness and the GSR readings or the LSTM autoencoder's processing of GSR data, the autoencoder model nonetheless holds potential. It demonstrates an ability to discern patterns within the physiological data which, with further research and refinement, could lead to more accurate predictors of motion sickness. The value of the autoencoder lies in its capacity to analyse complex, time-series data and identify anomalies that, although not yet statistically correlated with self-reported motion sickness, may still be relevant indicators of the condition's onset. Future work will aim to harness this capability more effectively, perhaps by incorporating additional data sources or refining the model's

architecture, to realize a robust tool for predicting motion sickness in virtual environments.

In future studies, more advanced simulators with novel motion cueing algorithms will be utilized for experimentation and data collection to evaluate VIMS and simulator sickness [30]–[32].

#### Acknowledgment

The authors would like to acknowledge the support of Australian Research Council (Project ID: DE210101623) and IISRI, Deakin University for providing required equipment and Labs to successfully conduct this project.

#### REFERENCES

- [1] R. S. Kennedy, J. Drexler, and R. C. Kennedy, "Research in visually induced motion sickness," *Appl. Ergon.*, vol. 41, no. 4, pp. 494–503, 2010, doi: 10.1016/j.apergo.2009.11.006.
- [2] B. Keshavarz, B. E. Riecke, L. J. Hettinger, and J. L. Campos, "Vection and visually induced motion sickness: How are they related?," *Front. Psychol.*, vol. 6, no. APR, 2015, doi: 10.3389/fpsyg.2015.00472/ABSTRACT.
- [3] L. Kooijman, H. Asadi, S. Mohamed, and S. Nahavandi, "A Virtual Reality Study Investigating the Effect of Cybersickness on the Relationship Between Vection and Presence Across Environments with Varying Levels of Ecological Relevance," *Int. Conf. Hum. Syst. Interact. HSI*, vol. 2022-July, pp. 1–8, 2022, doi: 10.1109/HSI55341.2022.9869507.
- [4] G. Bertolini and D. Straumann, "Moving in a moving world: A review on vestibular motion sickness," *Frontiers in Neurology*, vol. 7, no. FEB. Frontiers Media S.A., p. 14, Feb. 15, 2016, doi: 10.3389/fneur.2016.00014.
- [5] B. Keshavarz and H. Hecht, "Validating an Efficient Method to Quantify Motion Sickness," *Hum. Factors J. Hum. Factors Ergon. Soc.*, vol. 53, no. 4, pp. 415–426, Aug. 2011, doi: 10.1177/0018720811403736.
- [6] J. E. Bos, W. Bles, and E. L. Groen, "A theory on visually induced motion sickness," *Displays*, vol. 29, no. 2, pp. 47–57, Mar. 2008, doi: 10.1016/j.displa.2007.09.002.
- [7] A. Koohestani *et al.*, "A Knowledge Discovery in Motion Sickness: A Comprehensive Literature Review," *IEEE Access*, vol. 7, pp. 85755–85770, 2019, doi: 10.1109/ACCESS.2019.2922993.
- [8] Y. H. Cha *et al.*, "Motion sickness diagnostic criteria: Consensus Document of the Classification Committee of the Bárány Society," *J. Vestib. Res. Equilib. Orientat.*, vol. 31, no. 5, pp. 327–344, 2021, doi: 10.3233/VES-200005.
- [9] N. Umatheva, F. Russo, and B. Keshavarz, "Exploring the Association Between Lifestyle Factors and Visually Induced Motion Sickness," *Proc. Hum. Factors Ergon. Soc. Annu. Meet.*, vol. 66, no. 1, pp. 1013–1014, 2022, doi: 10.1177/1071181322661459.
- [10] B. Keshavarz, B. Murovec, N. Mohanathas, and J. F. Golding, "The Visually Induced Motion Sickness Susceptibility Questionnaire (VIMSSQ): Estimating Individual Susceptibility to Motion Sickness-Like Symptoms When Using Visual Devices," *Hum. Factors J. Hum. Factors Ergon. Soc.*, p. 001872082110086, 2021, doi: 10.1177/00187208211008687.
- [11] O. X. Kuiper, J. E. Bos, and C. Diels, "Vection does not necessitate visually induced motion sickness," *Displays*, vol. 58, no. October 2018, pp. 82–87, 2019, doi: 10.1016/j.displa.2018.10.001.
- [12] N. Duzmanska, P. Strojny, and A. Strojny, "Can simulator sickness be avoided? A review on temporal aspects of simulator sickness," *Frontiers in Psychology*, vol. 9, no. NOV. Frontiers Media S.A., Nov. 06, 2018, doi: 10.3389/fpsyg.2018.02132.
- [13] S. Sharples, S. Cobb, A. Moody, and J. R. Wilson, "Virtual reality induced symptoms and effects (VRISE): Comparison of head mounted display (HMD), desktop and projection display systems," *Displays*, vol. 29, no. 2, pp. 58–69, Mar. 2008, doi: 10.1016/j.displa.2007.09.005.

- [14] T. Irmak, D. M. Pool, and R. Happee, "Objective and subjective responses to motion sickness: the group and the individual," *Exp. Brain Res.*, vol. 1, p. 3, Nov. 2020, doi: 10.1007/s00221-020-05986-6.
- [15] H. Wan, S. Hu, and J. Wang, "Correlation of Phasic and Tonic Skin-Conductance Responses with Severity of Motion Sickness Induced by Viewing an Optokinetic Rotating Drum," *Percept. Mot. Skills*, vol. 97, no. 3, suppl, pp. 1051–1057, Dec. 2003, doi: 10.2466/pms.2003.97.3f.1051.
- [16] H. D. Nguyen, K. P. Tran, S. Thomassey, and M. Hamad, "Forecasting and Anomaly Detection approaches using LSTM and LSTM Autoencoder techniques with the applications in supply chain management," *Int. J. Inf. Manage.*, vol. 57, p. 102282, Apr. 2021, doi: 10.1016/j.ijinfomgt.2020.102282.
- [17] W. Al-Ashwal *et al.*, "Cybersickness Measurement and Evaluation during Flying a Helicopter in Different Weather Conditions in Virtual Reality," *Conf. Proc. - IEEE Int. Conf. Syst. Man Cybern.*, pp. 2152–2157, 2021, doi: 10.1109/SMC52423.2021.9659215.
- [18] R. Islam *et al.*, "Automatic Detection and Prediction of Cybersickness Severity using Deep Neural Networks from user's Physiological Signals," in *Proceedings - 2020 IEEE International Symposium on Mixed and Augmented Reality, ISMAR 2020*, 2020, pp. 400–411, doi: 10.1109/ISMAR50242.2020.00066.
- [19] N. Padmanaban, T. Ruban, V. Sitzmann, A. M. Norcia, and G. Wetzstein, "Towards a machine-learning approach for sickness prediction in 360° stereoscopic videos," *IEEE Trans. Vis. Comput. Graph.*, vol. 24, no. 4, pp. 1594–1603, Apr. 2018, doi: 10.1109/TVCG.2018.2793560.
- [20] L.-W. Ko *et al.*, "EEG-based motion sickness classification system with genetic feature selection," in *2013 IEEE Symposium on Computational Intelligence, Cognitive Algorithms, Mind, and Brain (CCMB)*, Apr. 2013, pp. 158–164, doi: 10.1109/CCMB.2013.6609180.
- [21] Y. Wang, J. R. Chardonnet, and F. Merienne, "VR sickness prediction for navigation in immersive virtual environments using a deep long short term memory model," *26th IEEE Conf. Virtual Real. 3D User Interfaces, VR 2019 - Proc.*, no. March, pp. 1874–1881, 2019, doi: 10.1109/VR.2019.8798213.
- [22] A. Krenker, J. Bester, and A. Kos, "Introduction to the Artificial Neural Networks," in *Artificial Neural Networks - Methodological Advances and Biomedical Applications*, InTech, 2011, pp. 1–18.
- [23] P. Malhotra, P., Vig, L., Shroff, G., & Agarwal, "Long Short Term Memory Networks for Anomaly Detection in Time Series," *ESANN 2015 proceedings, Eur. Symp. Artif. Neural Networks, Comput. Intell. Mach. Learn. Bruges (Belgium), 22-24 April 2015*, no. April, pp. 1–650, Jan. 2015.
- [24] S. Alsanwy, H. Asadi, M. Reza, C. Qazani, and S. Mohammed, "Prediction of Vehicle Motion Signals for Motion Simulators Using a Multivariate CNN-LSTM Model," 2023, no. November.
- [25] S. Alsanwy, H. Asadi, M. R. C. Qazani, S. Mohamed, and S. Nahavandi, "A CNN-LSTM Based Model to Predict Trajectory of Human-Driven Vehicle," in *2023 IEEE International Conference on Systems, Man, and Cybernetics (SMC)*, Oct. 2023, pp. 3097–3103, doi: 10.1109/SMC53992.2023.10394243.
- [26] S. Alsanwy, M. R. C. QAZANI, W. Al Ashwal, A. Shajari, S. Nahavandi, and H. Asadi, "Vehicle Trajectory Prediction Using Deep Learning for Advanced Driver Assistance Systems and Autonomous Vehicles," 2024.
- [27] W. Yu, C. Mechefske, and I. I. Y. Kim, "Time Series Reconstruction Using a Bidirectional Recurrent Neural Network based Encoder-Decoder Scheme," in *AIAC - 18th Australian International Aerospace Congress (AIAC2018); HUMS - 11th Defence Science and Technology (DST) International Conference on Health and Usage Monitoring (HUMS 2019); ISSFD - 27th International Symposium on Space Flight Dynamics (ISSFD)*, 2019, pp. 1–9.
- [28] M. Sakurada and T. Yairi, "Anomaly detection using autoencoders with nonlinear dimensionality reduction," *ACM Int. Conf. Proceeding Ser.*, vol. 02-December, pp. 4–11, 2014, doi: 10.1145/2689746.2689747.
- [29] R. S. Kennedy, N. E. Lane, K. S. Berbaum, and M. G. Lilienthal, "Simulator Sickness Questionnaire: An Enhanced Method for Quantifying Simulator Sickness," *Int. J. Aviat. Psychol.*, vol. 3, no. 3, pp. 203–220, Jul. 1993, doi: 10.1207/s15327108ijap0303\_3.
- [30] M. R. C. Qazani, H. Asadi, T. Bellmann, S. Perdrammehr, S. Mohamed, and S. Nahavandi, "A new fuzzy logic based adaptive motion cueing algorithm using parallel simulation-based motion platform," *IEEE Int. Conf. Fuzzy Syst.*, vol. 2020-July, 2020, doi: 10.1109/FUZZ48607.2020.9177599.
- [31] M. R. C. Qazani, H. Asadi, and S. Nahavandi, "An Optimal Motion Cueing Algorithm Using the Inverse Kinematic Solution of the Hexapod Simulation Platform," *IEEE Trans. Intell. Veh.*, vol. 7, no. 1, pp. 73–82, 2022, doi: 10.1109/TIV.2021.3068286.
- [32] H. Asadi, T. Bellmann, M. C. Qazani, S. Mohamed, C. P. Lim, and S. Nahavandi, "A Novel Decoupled Model Predictive Control-Based Motion Cueing Algorithm for Driving Simulators," *IEEE Trans. Veh. Technol.*, vol. 72, no. 6, pp. 7024–7034, 2023, doi: 10.1109/TVT.2023.3237317.